Origin of depolarized light scattering in supercooled liquids: Orientational fluctuation versus induced scattering mechanisms

H.Z. Cummins, Gen Li, and Weimin Du
Physics Department, City College of the CUNY, New York, New York 10031

Robert M. Pick and Catherine Dreyfus
Laboratoire de Dynamique de la Matière Condensée, Universite Pierre et Marie Curie, 75230 Paris Cedex 05, France*
(Received 5 July 1995)

Depolarized light scattering spectra of liquid salol that have been analyzed in recent studies of the liquid-glass transition are reexamined in order to determine the relative importance of orientational fluctuations and interaction-induced scattering. First, the spectra of CCl_4, $CHCl_3$, CH_2Cl_2, and CS_2 for which all the relevant parameters are known are compared to theoretical predictions in order to verify the experimental procedure. The same procedure is then applied to the molecular glass former salol for which we find that orientational fluctuations dominate at all frequencies up to at least 4000 GHz. We suggest that the previously reported agreement between depolarized light scattering spectra and predictions of the mode coupling theory for salol and other molecular glass forming materials results from coupling between rotational and translational motions of the molecules.

PACS number(s): 64.70.Pf, 78.35.+c, 61.25.Em

I. INTRODUCTION

Depolarized light scattering spectroscopy of supercooled liquids has been employed by several groups in recent years as part of a concerted effort to elucidate the dynamical mechanism underlying the liquid-glass transition [1–8]. These spectra have been interpreted for some materials as arising primarily from an interaction-induced scattering mechanism [dipole-induced-dipole (DID) mechanism], which allowed the observed spectra to be related directly to the dynamics of density fluctuations [9,10] and thus compared to predictions of the mode coupling theory (MCT) of the liquid-glass transition [11,10]. These light scattering spectra have been found to exhibit many of the detailed characteristics predicted by MCT and, together with inelastic neutron scattering data, have provided strong support for the relevance of the MCT to real glass forming materials.

Despite the success of this approach, several central questions related to these experiments have not yet been resolved. In this paper, we explore the relative contributions to these spectra of two light scattering mechanisms: interaction-induced scattering and orientational fluctuations.

Low-frequency depolarized light scattering from liquids has three principal origins: shear modes (which are the transverse acoustic modes at low temperatures), orientational fluctuations, and interaction-induced scattering. Shear mode scattering can be eliminated by using the backscattering geometry [12], orientational fluctuations are only relevant for anisotropic molecules, while interaction-induced scattering always occurs. In liquids containing anisotropic molecules or ions, orientational and interaction-induced scattering both occur even in depolarized backscattering and cannot be separated by any purely experimental procedure.

Since many of the glass forming materials investigated in recent light scattering studies contain anisotropic molecules or ions, it is important to determine the extent to which each of the two scattering mechanisms contributes to the observed spectra. [This problem was noted in Ref. [1], where spectra of the glass forming mixed salt calcium potassium nitrate (CKN) were compared with spectra of mixed KCl-$ZnCl_2$, which presumably produces no orientational contribution, and were found to be qualitatively similar.] While the relative importance of the two scattering mechanisms has been investigated previously for several simple liquids [13,14], no quantitative comparison of the two contributions has yet been carried out for glass forming materials, a comparison that is particularly critical for highly anisotropic molecular glass formers such as salol. Incidentally, we note that in two previous studies of light scattering from liquid CS_2, one [15] attributed the depolarized scattering entirely to orientational fluctuations, while the other [16] attributed it to interaction induced (DID) scattering. It has also been proposed that depolarized light scattering spectra of anisotropic molecular fluids may have a "narrow" component associated with orientational dynamics and a "broad" component due to interaction-induced scattering [17].

In Sec. II we review the theoretical predictions for the two scattering mechanisms and previous experimental and computer simulation data. In Sec. III we first test our experimental technique for deciding which scattering mechanism is dominant by studying three closely related

*ERS F0115 du CNRS.

materials, CCl_4, $CHCl_3$ and CH_2Cl_2, as well as CS_2, four systems for which a comparison with theory can be made because all the physical constants are known. Our results on CS_2 and CCl_4 allow us to make contact with earlier experiments on CS_2 [15,16] and with an earlier molecular dynamics comparison of the spectra of these two substances by McTague *et al.* [18]. We then present data on the molecular glass forming material salol and on solutions of salol in CCl_4. In Sec. IV we discuss the dynamics underlying the observed light scattering spectra of molecular glass formers such as salol and the relation of the spectra to the predictions of MCT.

II. LIGHT SCATTERING MECHANISMS

A. Orientational fluctuations

Consider a volume V filled with identical molecules at number density N, each with isotropic atomic polarizability α, illuminated by a monochromatic incident plane wave (intensity I_I, electric field $\vec{E}_I = E_I \hat{n}_I$, angular frequency ω_I, and wave vector k_I). Scattered light of intensity I_S, electric field $\vec{E}_S = E_S \hat{n}_S$, produced by the atomic dipoles is detected at a (large) distance r from the scattering volume. For scattering in the plane perpendicular to $\vec{E}_I$, assuming that the molecular positions are uncorrelated ($N\lambda^3 \ll 1$), the scattered intensity I_S is

$$I_S = NV\, I_I k^4 \alpha^2 / r^2 \ , \tag{2.1}$$

with $\vec{E}_S$ parallel to $\vec{E}_I$ (Rayleigh scattering).

For comparison with experiment, I_S is usually scaled by $I_I V/r^2$ to produce a geometry-independent cross section per unit volume (or Rayleigh ratio) R with dimensions (cm^{-1})

$$R = \frac{I_S r^2}{I_I V} \ . \tag{2.2}$$

For the case in Eq. (2.1) of isotropic uncorrelated molecules and scattering at 90° from the incident beam, the Rayleigh ratios for scattered light polarized perpendicular (V) or parallel (H) to the scattering plane (k_I, k_S) are

$$R_{VV} = Nk^4\alpha^2 \ , \tag{2.3}$$

$$R_{VH} = 0 \ . \tag{2.4}$$

For anisotropic molecules, the polarizability is a tensor property. The average scattered intensity $\langle I_S \rangle$ and spectrum $I_S(\omega)$ are determined by the scattered field correlation function [19]

$$\begin{aligned} C_{IS}(t) &= \langle E_S(t) E_S(0) \rangle \\ &= (E_I^2 k^4 / r^2) \left\langle \sum_{j=1}^{N} \alpha^j_{IS(t)} e^{iq\cdot r_j(t)} \right. \\ &\quad \left. \times \sum_{m=1}^{N} \alpha^m_{IS(0)} e^{iq\cdot r_m(0)} \right\rangle \ , \end{aligned} \tag{2.5}$$

where $\alpha^j_{IS} = \hat{n}_I \cdot \boldsymbol{\alpha}^j \cdot \hat{n}_S$ and $\vec{q} = \vec{k}_S - \vec{k}_I$ is the scattering vector.

Computer simulations and experiments [13] show that for depolarized scattering (i.e., VH geometry) in pure molecular fluids, the cross terms in Eq. (2.5) make only a small contribution compared to the "self" terms, so that, to a good approximation,

$$C_{IS}(t) \propto \left\langle \sum_j \alpha^j_{IS}(t) \alpha^j_{IS}(0) e^{iq\cdot[r_j(t) - r_j(0)]} \right\rangle \ . \tag{2.6}$$

For simplicity we will assume that the molecules are axially symmetric so that the polarizability tensor is given by

$$\boldsymbol{\alpha} = \begin{pmatrix} \alpha_\parallel & 0 & 0 \\ 0 & \alpha_\perp & 0 \\ 0 & 0 & \alpha_\perp \end{pmatrix} \ . \tag{2.7}$$

We define the mean polarizability α by

$$\alpha = \frac{1}{3}(\alpha_\parallel + 2\alpha_\perp) \tag{2.8a}$$

and the anisotropy β by

$$\beta = (\alpha_\parallel - \alpha_\perp) \ . \tag{2.8b}$$

The total depolarized Rayleigh ratio R_{VH} due entirely to the anisotropy is given by [19]

$$R_{VH} = Nk^4 (\tfrac{1}{15}\beta^2) \ , \tag{2.9}$$

while the polarized Rayleigh ratio R_{VV} is given by

$$R_{VV} = R_{\mathrm{iso}} + \frac{4}{3} R_{VH} \ , \tag{2.10}$$

where R_{iso} is determined by the isotropic part of the polarizability tensor and is therefore independent of rotations. For gases, where the molecular positions are uncorrelated, R_{iso} is given by Eq. (2.3), where α is the average polarizability, given by Eq. (2.8a). In this case the integrated depolarization ratio

$$\rho = \frac{I_{VH}}{I_{VV}} = \frac{R_{VH}}{R_{VV}} \tag{2.11}$$

is given by

$$\rho_{\mathrm{gas}} = \frac{(\beta^2/15)}{\alpha^2 + 4\beta^2/45} = \frac{3(\alpha_{11} - \alpha_\perp)^2}{5(\alpha_{11} + 2\alpha_\perp)^2 + 4(\alpha_{11} - \alpha_\perp)^2} \ . \tag{2.12a}$$

[Equation (2.12a) can be used to find β from measurements of ρ in gases.]

In liquids, where $N\lambda^3 \gg 1$, R_{iso} is reduced by interference effects, typically by a factor of 10 – 100 relative to Eq. (2.3). As first shown by Einstein, the integrated intensity R_{iso} for fluids results from density fluctuations and can be computed as [20]

$$R^{\mathrm{fl}}_{\mathrm{iso}} = \frac{\pi^2}{\lambda_0^4} k_B T (n^2 - 1)^2 \kappa_T \ , \tag{2.12b}$$

where κ_T is the isothermal compressibility. For liquids, we therefore take

$$R_{VV}^{\text{th}} = R_{\text{iso}}^{\text{fl}} + \frac{4}{3}R_{VH} \ . \tag{2.13}$$

The reduction in R_{iso} also leads to depolarization ratios for liquids that are usually much larger than for the corresponding gases.

The spectral depolarization ratio

$$\rho(\omega) = \frac{I_{VH}(\omega)}{I_{VV}(\omega)} \tag{2.14}$$

is strongly frequency dependent. For simple liquids, $I_{\text{iso}}(\omega)$ appears as a narrow triplet consisting of a central quasielastic thermal diffusion component plus two symmetrically shifted Brillouin components [21]. In this spectral range, $\rho(\omega)$ may be very small. But for frequencies beyond the range of $I_{\text{iso}}(\omega)$, both $I_{VV}(\omega)$ and $I_{VH}(\omega)$ display the same broad "rotational wing" and $\rho(\omega) = \frac{3}{4}$ *independent* of the relative anisotropy β/α.

B. Interaction-induced scattering

Since the observation of a broad depolarized component in the light scattering spectra of monatomic gases (for which $\beta = 0$) by McTague and Birnbaum in 1968 [22], the study of interaction-induced (or collision-induced) light scattering in liquids and gases has been pursued by many investigators [23]. While several different interaction-induced scattering mechanisms exist [24], the most important one for dense liquids is the dipole-induced-dipole mechanism, first discussed by Silberstein in 1917 [25]. In the DID picture, the dipole moment $\vec{p}_i$ induced on a molecule i by the incident light in turn polarizes its neighbors, which then radiate at the same frequency. The fluctuations of the total dipole of the sample produces the scattered DID intensity.

For simplicity, we will ignore optical anisotropy and let each molecule have isotropic polarizability α. A molecule at $\vec{r}_i$, polarized by the incident field $\vec{E}_I$, will have a dipole moment $\vec{p} = \alpha \vec{E}_I$. The electric field at $\vec{r}_j$ due to this dipole is [26]

$$\vec{E}_D^{\,i}(\vec{r}_j) = \frac{3\hat{n}(\vec{p}\cdot\hat{n}) - \vec{p}}{|\vec{r}_i - \vec{r}_j|^3} \ , \tag{2.15}$$

where $\hat{n}$ is a unit vector from $\vec{r}_i$ towards $\vec{r}_j$. The γ component of the total dipole field at $\vec{r}_j$ due to all such $\vec{r}_i$ molecules (neglecting retardation effects) is given by

$$E_D^{\gamma} = \sum_{j\neq i} \alpha T^{\gamma\beta}(r_{ij}) E_I^{\beta} \ , \tag{2.16}$$

where

$$T^{\gamma\beta}(r) = \frac{1}{r^3}(3\hat{r}_\gamma \hat{r}_\beta - \delta_{\gamma\beta}) \ . \tag{2.17}$$

If a small volume element $V \ll \lambda^3$ contains NV identical molecules, then the total far-field polarized scattered intensity I_{VV}^{DID} due to the polarization induced on each molecule by the dipole field (2.16) is

$$I_{VV}^{\text{DID}} = \frac{k^4}{r^2} I_I \alpha^4 \left(\sum_{i,j=1}^{NV}{}' T^{ZZ}(r_{ij}) \right)^2 \tag{2.18}$$

and the corresponding depolarized intensity is $I_{VH}^{\text{DID}} = \frac{3}{4} I_{VV}^{\text{DID}}$.

The sum in Eq. (2.18) depends on the positions of all NV molecules and cannot generally be calculated analytically. (For high-symmetry distributions, the sum vanishes identically.) Therefore, molecular dynamics simulations (e.g., [27,28]) have been employed to calculate the sums. Bykhovskii and Pick [28] find that for a Lennard-Jones liquid at zero pressure, at densities near the glass transition,

$$\frac{\sigma^6}{NV} \left(\sum_{i,j=1}^{NV}{}' T^{ZZ}(r_{ij}) \right)^2 \sim 0.25$$

while $N\sigma^3 \sim 1$, so that the DID intensity per molecule is

$$I_{VV}^{\text{DID}}(NV) \simeq \frac{k^4}{r^2} I_I \alpha^4 \times 0.25 N^2 \ . \tag{2.19}$$

Therefore, for a macroscopic scattering volume ($V \gg \lambda^3$), assuming random phases for the scattered fields from different volume elements, the corresponding DID Rayleigh ratios are

$$R_{VV}^{\text{DID}} \approx N^3 k^4 \alpha^4 \times 0.25 \ , \tag{2.20a}$$

$$R_{VH}^{\text{DID}} \approx N^3 k^4 \alpha^4 \times 0.19 \ . \tag{2.20b}$$

(Note that the depolarization ratio $\rho_{\text{DID}} = 0.75$ is the same as the result for orientational fluctuations at frequencies above the range of I_{iso}.)

From Eqs. (2.20a) and (2.10), the ratio of the intensities of DID scattering to orientational fluctuation scattering (rot) for I_{VV} is approximately

$$\frac{I_{VV}^{\text{DID}}}{I_{VV}^{\text{rot}}} = \frac{45}{4} \times \frac{\alpha^4 N^2}{(\alpha_{11} - \alpha_\perp)^2} \times 0.25 = \frac{2.8\alpha^4 N^2}{(\alpha_{11} - \alpha_\perp)^2} \ . \tag{2.21}$$

(The same result applies to I_{VH}.) The numerical factor 2.8 in Eq. (2.21) is approximate, but can easily be refined using the data in [28].

In deriving Eq. (2.21) we have assumed that the DID and rotational contributions are independent. Computer simulations for anisotropic molecules indicate that small cross terms exist as well [13,14], but we will not consider these terms here. As shown by Frenkel and McTague [13], molecular dynamics simulations for N_2 and CO_2 indicate that the orientational and DID spectra are similar in form and that the orientational contribution dominates at all frequencies out to $\sim 300\ \text{cm}^{-1}$.

C. Numerical evaluations

In principle, Eq. (2.21) should be sufficient to determine which scattering mechanism, DID or rotational, is dominant for glass forming liquids such as salol. Assuming that cross terms between orientational and DID polarization can be neglected, all that is needed is the number density N, the mean polarizability α, and the polarizability anisotropy β. Unfortunately, β has not been measured for salol or any of the common glass forming materials (e.g., CKN, OTP, and glycerol). We have therefore followed an indirect route in order to determine the dominant scattering mechanism for salol.

First we measured the VV and VH spectra of the molecular liquids CCl_4, $CHCl_3$, CH_2Cl_2, and CS_2 for which N, α, and β are known. From the integrated spectra we found the corresponding Rayleigh ratios and compared them with the theoretical predictions of Sec. II. Reasonably good agreement was obtained, indicating that the method is applicable. We then measured the VV and VH spectra of salol as well as of salol dissolved in CCl_4. As described below, the results show that orientational fluctuations are the principal source of light scattering for salol.

Measurements of R and ρ have been reported for many liquids and gases; for liquids, typical experimental values for R_{VV} are $\sim 1 \times 10^{-5}$ cm^{-1} [29–31]. Much of the data up to 1962 had been summarized by Fabelinskii [29]. The older literature is often unreliable, however, partly because vibrational Raman scattering was often inadvertently included and partly because the limited sensitivity available before the advent of lasers made R_{VH} and ρ difficult to measure accurately, particularly in gases. The average polarizability α is usually determined from measurements of the refractive index n via the Lorentz-Lorenz equation [32]

$$\alpha = \frac{3}{4\pi N}\frac{n^2-1}{n^2+2}\,, \tag{2.22}$$

while β is determined either from Kerr constant measurements or from depolarization measurements performed in the gas phase [29].

In Table I we list values of α for the five materials studied, obtained with Eq. (2.22) using handbook values [33] for the refractive index n and number intensity N. Polarizability anisotropy values β and depolarization ratios ρ for CCl_4, $CHCl_3$, and CH_2Cl_2 are from the depolarized light scattering measurements of Bridge and Buckingham [34], while for CS_2 both α and β are from Bogaard and Orr [35].

The second section of Table I lists the theoretical Rayleigh ratios predicted for these materials in the liquid phase at 20 °C, taking $\lambda = 2\pi/k = 4880$ Å. The $R_{\rm iso}^{\rm fl}$ values were computed using published κ_T values for CCl_4, $CHCl_3$, and CS_2, while for CH_2Cl_2 and salol κ_T was approximated by values obtained from the Brillouin shifts and previously determined sound velocities. The third entry in this section gives R_{VV}, assuming that the VH spectrum is rotational in origin, as shown by the first entry ($R_{VH}^{\rm rot}$). The last entry in this section shows the calculated intensity ratio $I^{\rm DID}/I^{\rm rot}$ (or $R^{\rm DID}/R^{\rm rot}$), which applies for either VH or VV. Note that this ratio is > 16 for CCl_4 so that interaction-induced (DID) scattering should predominate (as expected), while for the other materials the ratio is ≤ 0.12, indicating that orientational fluctuations should dominate. Finally, in the last section of Table I, we include experimental R_{VV} and ρ values for CCl_4, $CHCl_3$, and CS_2. Since we did not measure absolute intensities in our experiments, we arbitrarily adopted the value $R_{VV}(CHCl_3) = 1.0 \times 10^{-5}$ (cm^{-1}) as a standard in the analysis of our data presented in Sec. III.

Since the frequency dependence of $R^{\rm DID}$ and $R^{\rm rot}$ has not been analyzed for the materials we are studying here, it could be possible that $R^{\rm rot}$ dominates at low frequencies while $R^{\rm DID}$ becomes important at higher frequencies. Frenkel and McTague [13] reported molecular dynamics studies of $R^{\rm DID}$ and $R^{\rm rot}$ for N_2 and CO_2 and found that

TABLE I. Theoretical and experimental Rayleigh ratios (cm^{-1}).

Quantity	CCl_4	$CHCl_3$	CH_2Cl_2	CS_2	$C_{13}H_{10}O_3$
$\rho_{\rm exp}$ (gas)	$< 5 \times 10^{-5}$ [34]	0.625×10^{-2} [34]	1.124×10^{-2} [34]	0.072 (from α and β)	
α (cm^3) [Eq. (2.22)]	10.5×10^{-24}	8.5×10^{-24}	6.44×10^{-24}	8.6×10^{-24} [35]	2.24×10^{-24}
$\beta = (\alpha_\parallel - \alpha_\perp)$	$< 2.8 \times 10^{-25}$ (from α and ρ)	2.6×10^{-24} (from α and ρ)	2.66×10^{-24} (from α and ρ)	9.4×10^{-24} [35]	
κ_T (10^{-12} cm^2/dyn)	106 [46]	101 [46]	65 [47]	93 [46]	36 [47]
Theory (liquid)					
$R_{VH}^{\rm rot}$ [Eq. (1.5b)]	$< 9.6 \times 10^{-9}$	9.3×10^{-7}	1.2×10^{-6}	1.6×10^{-5}	
$R_{\rm iso}^{\rm fl}$ [Eq. (2.12b)]	9.6×10^{-6}	8.7×10^{-6}	4.8×10^{-6}	1.85×10^{-5}	3.9×10^{-6}
R_{VV} [Eq. (2.13)]	9.8×10^{-6}	9.9×10^{-6}	6.4×10^{-6}	4.0×10^{-5}	
$R_{VH}^{\rm DID}$ [Eq. (2.20b)]	1.54×10^{-7}	1.17×10^{-7}	7.46×10^{-8}	2.85×10^{-7}	5.83×10^{-11}
$\frac{4}{3}R_{VH}^{\rm DID}/R_{\rm iso}$	0.021	0.018	0.021	0.021	2×10^{-5}
$R^{\rm DID}/R^{\rm rot}$ [(Eq. 2.21)]	$> 16.$	0.12	0.06	0.02	
Expt. (liquid)					
$\rho_{\rm expt}$	0.0195 [45]	0.114 [45]		0.502 [45]	
$R_{VV}^{\rm expt}$	5.88×10^{-6} [30]	18.6×10^{-6} [29]		83.9×10^{-6} [31]	
	12.5×10^{-6} [29]			77×10^{-6} [29]	

R^{rot}/R^{DID} is uniformly > 1 and is nearly frequency independent. Kivelson [17] has suggested that this result may not apply to large molecules such as salol for which rotational dynamics are slower, leading to a "separation of time scales" and a crossover to DID-dominated scattering at high frequencies. We will return to this point in the next section.

III. LIGHT SCATTERING EXPERIMENTS

A. CCl_4, $CHCl_3$, CH_2Cl_2, and CS_2

As noted in Sec. II C, we first performed light scattering experiments on liquid CCl_4, $CHCl_3$, CH_2Cl_2, and CS_2 in order to test the theoretical predictions of the

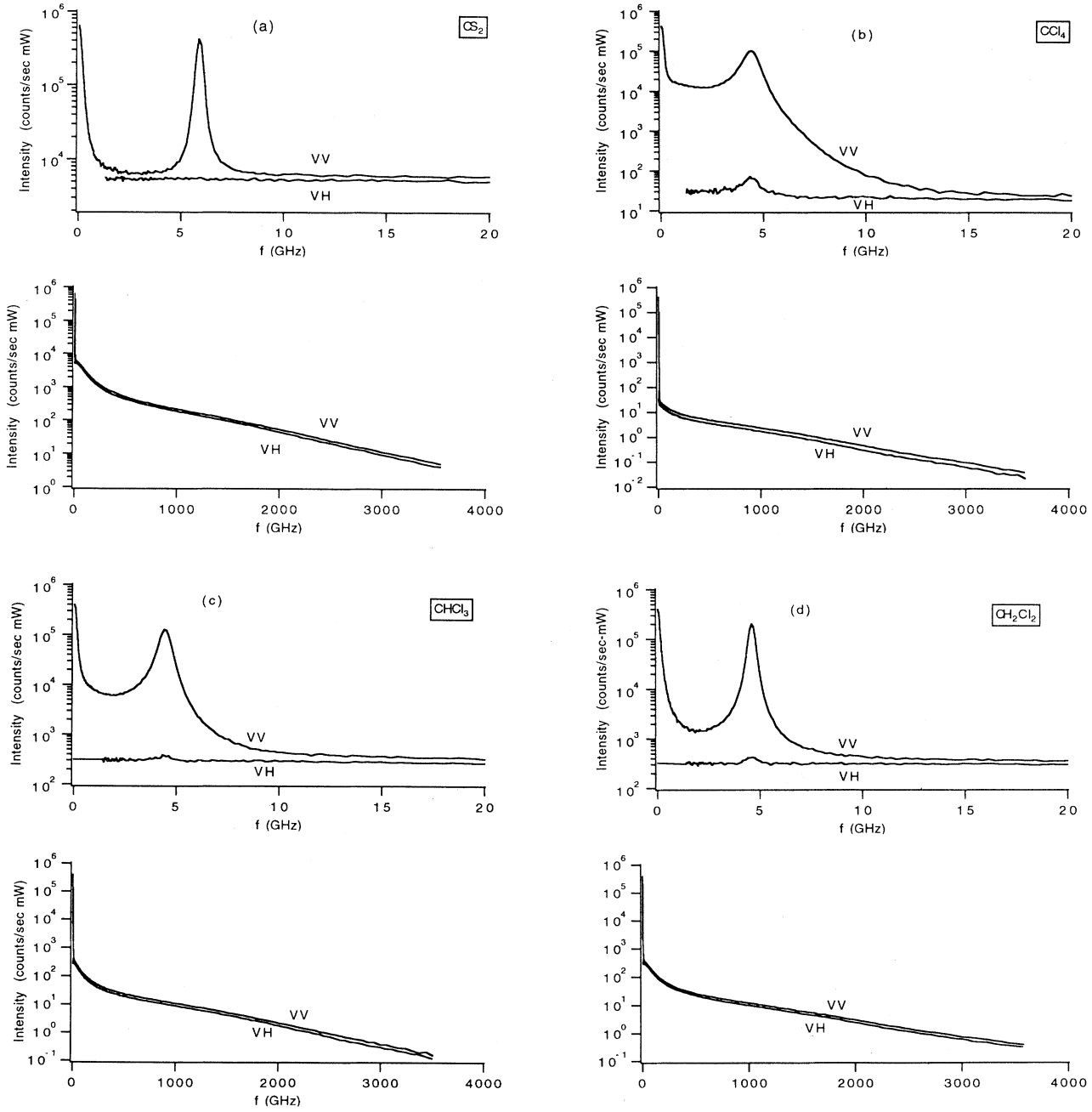

FIG. 1. Light scattering spectra of liquids at 300 K with 4880-Å excitation. Scattering angle $\theta = 90°$. Top, low-frequency VV and VH spectra; bottom, complete VV and VH spectra. (a) CS_2, (b) CCl_4, (c) $CHCl_3$, (d) CH_2Cl_2, and (e) salol.

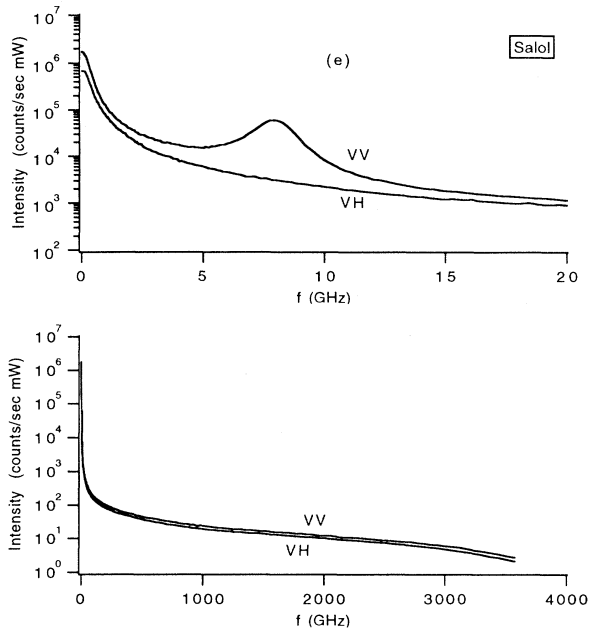

FIG. 1 *(Continued).*

relative importance, for each material, of the two light scattering mechanisms discussed in the preceding section. We subsequently applied the same procedure to salol. The liquids were filtered directly into 1-cm^2 square glass cuvettes and were studied at room temperature. $\theta = 90°$ VV and VH spectra excited with a 4880-Å argon laser were recorded with a Spex 1401 tandem grating spectrometer and with a Sandercock tandem Fabry-Pérot (FP) interferometer with several different mirror separation settings. The Stokes sides of the Raman and FP spectra were combined using the Raman intensities as reference, since these were collected with the most carefully controlled conditions. The resulting spectra normalized to the laser intensity, in counts/sec mW, were self-consistent to ±5%.

In order to determine the corresponding Rayleigh ratios, we integrated each spectrum from 0 to 3500 GHz to obtain a value of $I^{\rm tot}$ (counts/sec mW) that we compared to the result for the integrated $CHCl_3$ VV spectrum. Taking $R_{VV}(CHCl_3) = 1.0 \times 10^{-5}$ as a standard, this technique resulted in a conversion factor relating R to $I^{\rm tot}$: $R = 4.19 \times 10^{-11} \times I^{\rm tot}$.

The VV and VH spectra for CS_2 are shown in Fig. 1(a), plotted as $\log_{10}[I(\omega)]$ (counts/sec mW) vs f (GHz). The upper plot shows the low-frequency region ($0 \leq f \leq 20$ GHz) in which I_{VV} is dominated by the Rayleigh and Brillouin lines ($I_{\rm iso}$), whose peaks are ~ 100 times stronger than I_{VH}, which is flat in this region. The full VV and VH spectra are shown in the lower figure. For frequencies above ~ 10 GHz, I_{VV} and I_{VH} have identical line shapes with a constant depolarization ratio $\rho(\omega) \sim 0.75$. The corresponding spectra for CCl_4, $CHCl_3$, CH_2Cl_2, and salol are shown in Figs. 1(b), 1(c), 1(d), and 1(e), respectively.

Although for CS_2 the Rayleigh and Brillouin lines are much stronger than the depolarized background, their integrated intensity $I_{\rm iso} \equiv I_{VV}^{\rm low} - \frac{4}{3} I_{VH}^{\rm low}$ (where I^{LOW} indicates integration from 0 to 10 GHz only) is smaller than the integrated depolarized intensity. Numerical integration of the CS_2 spectra gave $I_{VH} = 9.1 \times 10^5$, $I_{VV} = 1.54 \times 10^6$, $I_{\rm iso} = 2.98 \times 10^5$, and $\rho = 0.59$. The ratio $I_{\rm iso}/I_{\rm ani}$ (where $I_{\rm ani} = \frac{4}{3} I_{VH}$) is 0.25 [36].

In Table II we list the integrated intensities for all five materials, converted to Rayleigh ratios by comparison with I_{VV} of $CHCl_3$. We also show the experimental values of $\frac{4}{3} R_{VH}/R_{\rm iso}$. Since both $R_{\rm iso}$ and the theoretical value of $\frac{4}{3} R_{VH}^{\rm DID}$ are independent of the anisotropy β and inclusion of orientational dynamics can only increase R_{VH}, the experimentally observed ratio $\frac{4}{3} R_{VH}/R_{\rm iso}$ should provide a good measure of the relative importance of the DID and orientational contributions. From Table I, the theoretical ratio $\frac{4}{3} R_{VH}^{\rm DID}/R_{\rm iso}$ for these materials (excluding salol) is uniformly ~ 0.02, while the experimental ratio $\frac{4}{3} R_{VH}/R_{\rm iso}$ increases from 0.03 for CCl_4 to 4.1 for CS_2, indicating that the DID mechanism is dominant only for CCl_4. This result is confirmed by the comparison of $R_{VH}^{\rm exp}$ with the predicted $R_{VH}^{\rm DID}$ and $R_{VH}^{\rm rot}$ shown at the bottom of Table II. For $CHCl_3$, CH_2Cl_2, and CS_2, $R_{VH}^{\rm exp}/R_{VH}^{\rm rot}$ is ~ 2, while $R_{VH}^{\rm exp}/R_{VH}^{\rm DID}$ is between 14 and 130. We therefore conclude that our experimental method and the theoretical evaluation of the DID Rayleigh ratio allow us to determine the origin of the

TABLE II. Experimental R and ρ values compared with theory.

Quantity	CCl_4	$CHCl_3$	CH_2Cl_2	CS_2	Salol
Expt. values [a]					
R_{VH}	2.2×10^{-7}	1.66×10^{-6}	2.02×10^{-6}	3.80×10^{-5}	1.76×10^{-5}
R_{VV}	9.2×10^{-6}	1×10^{-5} [b]	9.15×10^{-6}	6.45×10^{-5}	4.54×10^{-5}
$R_{\rm iso}$	8.8×10^{-6}	7.6×10^{-6}	6.3×10^{-6}	1.2×10^{-5}	2.1×10^{-5}
ρ	0.024	0.17	0.22	0.59	0.39
$\frac{4}{3} R_{VH}/R_{\rm iso}$	0.03	0.29	0.43	4.1	1.1
Comparison with theory					
$R_{VH}^{\rm expt}/R_{VH}^{\rm DID}$	1.4	14	27	130	3.0×10^5
$R_{VH}^{\rm expt}/R_{VH}^{\rm rot}$	> 23	1.8	1.7	2.4	

[a] Corrected for instrumental $I_V/I_H = 0.84$.

[b] Assumed value.

VH spectrum.

Note that the shape of $I(\omega)$ is not indicative of the origin of the VH spectrum. This is demonstrated in Fig. 2, where we show the VH spectra of CS_2 and CCl_4. (This figure is similar to Fig. 3 of McTague *et al.* [18].) The two spectra have very similar shapes with $I(CS_2) \sim 100I(CCl_4)$, yet we conclude from the last two lines of Table II that the CS_2 spectrum is primarily due to orientational fluctuations, while the CCl_4 spectrum is interaction induced. The fact that the two spectra nevertheless are qualitatively similar is consistent with the computer simulation results of Refs. [13] and [14].

B. Salol: Pure liquid and dilution experiments

For salol, as shown in Table II, the experimental R_{VH} value exceeds the theoretical DID value by a factor of $\sim 10^5$, indicating that the integrated anisotropic scattered intensity is overwhelmingly due to orientational fluctuations. The result for salol is more dramatic than for the other liquids, presumably because the large salol molecules are further apart, leading to a very small R^{DID} value. Note that at $T = 300$ K, salol is already supercooled by $\sim 20\,^{\circ}\mathrm{C}$, so that the main part of the VH orientational spectrum is much narrower than for the other liquids studied (see Fig. 1). Since the value of the dielectric anisotropy β of salol is not known, no theoretical comparison of R_{VH}^{rot} with R_{VH}^{exp} is possible. However, from Eq. (2.9) and R_{VH}^{exp}, an approximate value for β can be obtained: $\beta \sim 3.4 \times 10^{-24}$ cm^3, implying an anisotropy ratio $\beta/\alpha = 1.5$, somewhat larger than any of the other liquids in Table I.

In order to further explore the possible role of the DID mechanism for salol, we also studied the light scattering spectra of solutions of salol in CCl_4. (This experiment was motivated by a previous study of ortho-terphenyl by Patkowski and Steffen [37].) If the depolarized scattering from salol is due to orientation fluctuations, then the depolarized intensity for a salol-CCl_4 solution, above the (small) intrinsic CCl_4 intensity, should be equal to the observed intensity for pure salol multiplied by the ratio of number concentrations. Conversely, if the DID mechanism is responsible, then adding salol to CCl_4 should produce a *decrease* in $R_{VH}(\omega)$ according to the theoretical DID results shown in Table I. This experiment should therefore reveal a difference in the intensity relative to pure CCl_4 between high and low frequencies if there actually were a crossover between the two scattering mechanisms.

Figure 3 shows the observed VH spectra of CCl_4, salol, and a 10% salol-CCl_4 solution by weight. As seen in Fig. 3, the intensity of the 10% solution spectrum is well above that of the CCl_4 spectrum for all frequencies up to 4000 GHz, indicating that the salol spectrum is predominantly due to orientational fluctuations at all frequencies and that the intensity of DID scattering throughout this range is negligible for salol.

Finally, in Fig. 4 we show the three $\chi''(\omega)$ spectra computed from the $I_{VH}(\omega)$ spectra in Fig. 3 as $\chi''(\omega) = \omega I_{VH}(\omega)$. Comparing Figs. 3 and 4 shows that the increased intensity in $I(\omega)$ for the 10% solution relative to pure CCl_4 is not restricted to the α-peak region but is also seen in the high-frequency range of the spectra, which extends well beyond the region of the boson peak at ~ 500 GHz. Thus the idea of a crossover from low-frequency orientational scattering to high-frequency DID scattering mentioned in Sec. II appears to be ruled out for salol.

IV. DISCUSSION AND CONCLUSION

The analysis presented in Sec. III has shown that the depolarized light scattering spectrum measured by some of us in salol [38] arises predominantly from orientational fluctuations, a conclusion that seems likely to also apply to other molecular glass formers such as propylene car-

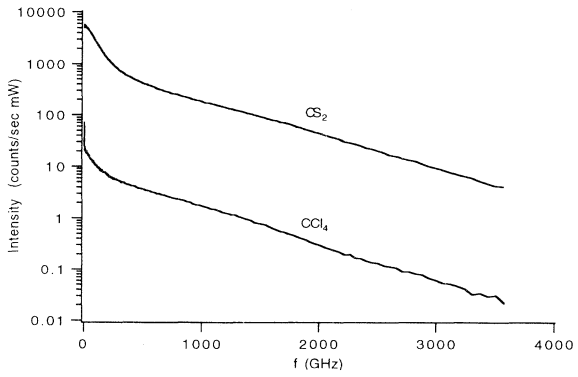

FIG. 2. VH spectra of CS_2 and CCl_4.

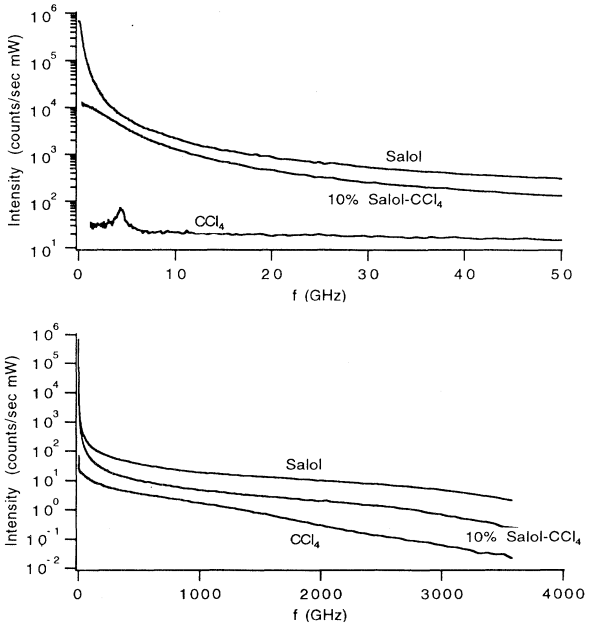

FIG. 3. VH spectra of CS_2, salol, and 10% salol-CCl_4 solution. Top, 0–50 GHz; bottom, 0–4000 GHz.

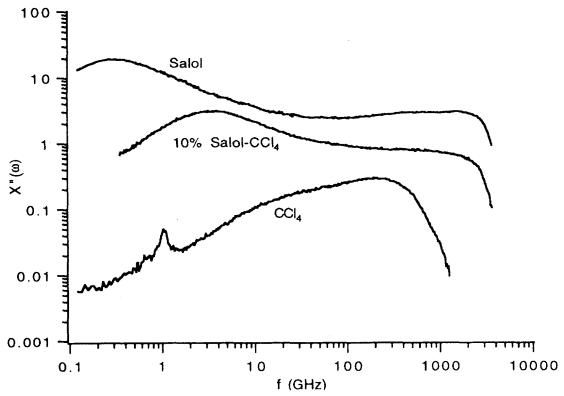

FIG. 4. VH $\chi''(\omega)$ spectra of salol, CCl_4, and 10% salol-CCl_4 solution.

bonate, orthoterphenyl, glycerol, or metatoluidine, for instance. In Ref. [38], this depolarized salol spectrum and its thermal evolution was analyzed using the $\chi''(\omega, T)$ predicted by the idealized MCT [11]. Consistent results were obtained and were subsequently refined [39] using an extended version of the MCT. Consistent results were also obtained with the idealized MCT when analyzing $\chi''(\omega)$ spectra of the molecular glass formers propylene carbonate [2], orthoterphenyl [5], glycerol [3], and more recently metatoluidine [8].

The preceding results represent a challenge for the theory. MCT has been developed as a theory of density fluctuation dynamics and the theoretical predictions of MCT apply directly to the density fluctuation correlators $\phi_q(t)$. These are the predictions that have been nevertheless compared sucessfully to the light scattering measurements. This success indicates that coupling between the orientational motion and the center of mass motion of the molecules is responsible for the similar dynamics of the orientational and density fluctuation correlators. Such a coupling has been extensively studied in molecular crystals possessing orientational disorder by different authors (including one of us [40]) and has been recently reviewed by Lynden-Bell and Michel [41]. However, for molecular crystals, the high symmetry of the crystals and of the molecules involved make the theoretical situation relatively easy to study. The absence of local symmetry in a molecular liquid and of the very small number of elements of the point group symmetry of the corresponding molecules makes the problem of applying the MCT in systems where this orientation-translation coupling must be taken into account a much more difficult problem to solve. It therefore remains to be shown that the orientational correlators exhibit the same properties as the density correlators. We note, however, that a molecular dynamics simulation of CKN by Signorini, Barrat, and Klein [42] provides important evidence supporting this conjecture. They computed the temperature-dependent susceptibility spectrum $\chi''(\omega)$ for the displacement of Ca^{2+} ions and found a temperature-dependent minimum. They also analyzed the orientational correlation function $C_2(t) = \langle P_2(\cos\theta)\rangle$ for the rotational dynamics of the NO_3^- ions. From $C_2(t)$ they computed the corresponding susceptibility $\chi_2''(\omega)$ and found that, at different temperatures, $\chi_2''(\omega)$ has a shallow minimum at approximately the same frequency as the minimum of the corresponding $\chi''(\omega)$ curve. The agreement between these two minima suggests that for CKN the orientational and translational dynamics are strongly coupled. This result agrees with the MCT prediction that close to T_C, in the region of the suceptibility minimum, the correlator of any variable that couples strongly to the density should have the same form as the density correlator $\phi_q(t)$ [11].

Finally, we note that Dixon *et al.* [43] have compared their salol dielectric data [44] with the depolarized light scattering data and found significant differences. This observation seems surprising in view of the fact that both the dielectric and light scattering spectra of salol probe the same orientational dynamics. However, dielectric measurements of polar molecular liquids probe the dynamics of orientable dipoles described by the correlation function $C_1(t) = \langle P_1(\cos\theta)\rangle$, while depolarized light scattering probes the dynamics of the anisotropic polarizability tensor described by $C_2(t) = \langle P_2(\cos\theta)\rangle$. While both techniques probe the same orientational dynamics, the detailed forms of these correlation functions, and thus of the corresponding susceptibility spectra, need not be the same. We will discuss this point further in a future work.

ACKNOWLEDGMENTS

We wish to thank W. Götze, K. Michel, W. Steffen, A. Patkowski, S.R. Nagel, N. Menon, M. Klein, and D. Kivelson for helpful discussions. R.M.P. thanks CUNY for financial support during a visit to New York. This research was supported by the NSF (Grant No. DMR-9315526), CNRS, and NATO Cooperative Research Grant No. CRG-930730.

[1] G. Li, W.M. Du, X.K. Chen, H.Z. Cummins, and N.J. Tao, Phys. Rev. A **45**, 3867 (1992) (CKN).

[2] W.M. Du, G. Li, H.Z. Cummins, M. Fuchs, J. Toulouse, and L.A. Knauss, Phys. Rev. E **49**, 2192 (1994) (propylene carbonate).

[3] J. Wuttke, J. Hernandez, G. Li, G. Coddens, H.Z. Cummins, F. Fujara, W. Petry, and H. Sillescu, Phys. Rev. Lett. **72**, 3052 (1994) (glycerol).

[4] M.J. Lebon, C. Dreyfus, G. Li, A. Aouadi, H.Z. Cummins, and R.M. Pick, Phys. Rev. E **51**, 4537 (1995) ($ZnCl_2$).

[5] W. Steffen, A. Patkowski, H. Glaser, G. Meier, and E.W. Fisher, Phys. Rev. E **49**, 2992 (1994) (OTP).

[6] E. Rossler, A.P. Sokolov, A. Kisliuk, and D. Quitmann, Phys. Rev. B **49**, 14 967 (1994) (tricresyl phosphate and glycerol).

[7] C. Alba-Simionesco and M. Krauzman, J. Chem. Phys. **102**, 6574 (1995) (m-toluidine).

[8] A. Aoudi, C. Dreyfus, M.J. Lebon, and C. Alba-Simionesco (unpublished) (m-toluidine).
[9] M.J. Stephen, Phys. Rev. **187**, 279 (1969).
[10] H.Z. Cummins, G. Li, W.M. Du, and J. Hernandez, Physica A **204**, 169 (1994).
[11] W. Götze and L. Sjögren, Rep. Prog. Phys. **55**, 241 (1992).
[12] Experimentally the shear mode contribution is much weaker than the other two, even in the 90° geometry used in this paper.
[13] D. Frenkel and J.P. McTague, J. Chem. Phys. **72**, 280 (1980).
[14] W.A. Steele, J. Mol. Liquids **48**, 321 (1991).
[15] S.L. Shapiro and H.P. Broida, Phys. Rev. **154**, 129 (1967).
[16] T.I. Cox and P.A. Madden, Mol. Phys. **39**, 1487 (1980).
[17] D. Kivelson and G. Tarjus, Phys. Rev. E **27**, 4210 (1993); D. Kivelson (private communication).
[18] J.P. McTague, P.A. Fleury, and D.B. Dupré, Phys. Rev. **188**, 303 (1969).
[19] B.J. Berne and R. Pecora, *Dynamic Light Scattering* (Wiley, New York, 1976).
[20] Equation (2.12b) is a frequently employed variant of the original Einstein formula in which $(\rho\frac{\partial\epsilon}{\partial\rho})$ is taken as $(\epsilon - 1)$. (See Ref. [31], p. 492.)
[21] While the spectrum $I_{\rm iso}(\omega)$ is q dependent, the integrated intensity given by Eq. (2.12b) does not depend on q.
[22] J.P. McTague and G. Birnbaum, Phys. Rev. Lett. **21**, 661 (1968).
[23] *Phenomena Induced by Intermolecular Interactions*, edited by G. Birnbaum (Plenum, New York, 1988).
[24] P.A. Madden, Mol. Phys. **36**, 365 (1978).
[25] L. Silberstein, Philos. Mag. **33**, 521 (1917).
[26] J.D. Jackson, *Classical Electrodynamics* (Wiley, New York, 1962).
[27] B.J. Alder, J.J. Weis, and H.L. Strauss, Phys. Rev. A **7**, 281 (1973).
[28] A.D. Bykhovskii and R.M. Pick, J. Chem. Phys. **100**, 7109 (1994).
[29] I.L. Fabelinskii, *Molecular Scattering of Light* (Plenum, New York, 1968).
[30] B. Chu, *Laser Light Scattering* (Academic, New York, 1974).
[31] M. Kerker, *The Scattering of Light* (Academic, New York, 1969).
[32] M. Born and E. Wolf, *Principles of Optics*, 2nd ed. (Macmillan, New York, 1964).
[33] *Handbook of Chemistry and Physics* (Chemical Rubber Company, Cleveland, 1979).
[34] N.J. Bridge and A.D. Buckingham, Proc. R. Soc. London Ser. A **295**, 334 (1966).
[35] M.P. Bogaard and B.J. Orr, in *Molecular Structure and Properties*, International Review of Science, Physical Chemistry Series Two, V2, edited by A.D. Buckingham (Butterworths, London, 1975), p. 149.
[36] This is smaller than the result $\frac{I_C+2I_B}{I_{\rm rot}} = 0.47$ found by Shapiro and Broida [15], possibly because our result was determined from the Stokes side only, where $I_{\rm ani}$ is larger than the anti-Stokes side.
[37] A. Patkowski and W. Steffen (private communication).
[38] G. Li, W.M. Du, A. Sakai, and H.Z. Cummins, Phys. Rev. A **46**, 3343 (1992) (salol).
[39] H.Z. Cummins, W.M. Du, M. Fuchs, W. Götze, A. Latz, G. Li, and N.J. Tao, Physica A **201**, 207 (1993).
[40] Ph. Buchet and R.M. Pick, J. Phys. (Paris) **48**, 821 (1987).
[41] R.M. Lynden-Bell and K.H. Michel, Rev. Mod. Phys. **66**, 721 (1994).
[42] G.F. Signorini, J.L. Barrat, and M.L. Klein, J. Chem. Phys. **92**, 1294 (1990).
[43] P.K. Dixon, N. Menon, and S.R. Nagel, Phys. Rev. E **50**, 1717 (1994).
[44] P.K. Dixon, L. Wu, S.R. Nagel, P.D. Williams, and J.P. Carini, Phys. Rev. Lett. **65**, 1108 (1990).
[45] R.C.C. Leite, R.S. Moore, and S.P.S. Porto, J. Chem. Phys. **40**, 3741 (1964).
[46] *American Institute of Physics Handbook*, 2nd ed. (McGraw-Hill, New York, 1963), pp. 2–177.
[47] Estimated from the frequency of Brillouin components and ultrasonic velocity data.